Est. 1984

ORIENTAL JOURNAL OF CHEMISTRY
An International Open Free Access, Peer Reviewed Research Journal

www.orientjchem.org

ISSN: 0970-020 X
CODEN: OJCHEG
2018, Vol. 34, No.(4):
Pg. 1749-1754

Electrochemical Analysis of the Anti-corrosion Properties of Benzonitrile Compound on Quenched 420 Martensitic Steel in Strong Aqueous Environment

ROLAND TOLULOPE LOTO[1]* and BRYAN UCHE AYOZIE[1]

[1]Department of Mechanical Engineering, Covenant University, Ota, Ogun State, Nigeria.
*Corresponding author E-mail: *tolu.loto@gmail.com

http://dx.doi.org/10.13005/ojc/340406

(Received: April 24, 2018; Accepted: July 14, 2018)

ABSTRACT

Investigation of the corrosion inhibition properties of benzonitrile compound on the surface degradation of quenched 420 martensitic steel in 6 M H_2SO_4 was evaluated through the application of potentiodynamic polarization method, micro analytical study and ATR-FTIR spectroscopic analysis. Experimental data showed optimal inhibition performance of the compound at peak inhibition efficiency of 99.4% with mixed type inhibition but dominant anodic inhibition properties. The inhibiting compound significantly influenced the thermodynamic behaviour of the steel resulting in chemisorption adsorption mechanism onto steel surface in consonance with Langmuir and Freundlich *adsorption isotherm* models with correlation coefficients of 1 and 0.7570. The transmittance of identified functional groups of benzonitrile from ATR-FTIR spectroscopy decreased at extended wavelengths due to surface coverage and adsorption of the compound onto the steel.

Keywords: Analysis, Anti-corrosion, Benzonitrile, Martensitic steel, Inhibitor.

INTRODUCTION

Stainless steels are metallic alloys with high corrosion resistance in comparison to carbon steels due to varying weight content of chromium, nickel etc. alloyed with the iron substrate metal. Martensitic grades of stainless steels exhibit superior mechanical properties and very low susceptibility to surface deterioration. They have extensive application in a wide range of industries where corrosion resistance and structural stability are of prime importance. 420 martensitic steel, an alteration of 410 steel, has slightly greater volumetric composition of carbon which enhances the hardness, strength and wear resistance of the steel. They basically derive their corrosion resistance from the presence of a passive protective film formed on their surfaces. Destruction of the film leads to localized corrosion deterioration and failures. 420 stainless steels are susceptible to corrosion in aqueous environments with high concentration of corrosive anions resulting. Their application in the presence of acids and aqueous solutions with aggressive anions progressively deteriorate their metallurgical properties.

Acids are extensively applied in numerous industrial technological processes such as; in pickling baths, industrial-equipment cleaning, pretreatments of compositions, extraction and processing of oil and gas and in chemical processing industries. Corrosion is a major problem in the petrochemical industries resulting in high maintenance cost[1-3]. Previous research on 420 steel concludes the overwhelming effect quenching on their corrosion resistance by as much as 60%[4]. Further increase in the versatility and application of 420 steels requires the use of chemical compounds (inhibitors) capable of inhibiting its corrosion in corrosive environments. Inhibitors control, reduce, or prevent electrochemical reactions between the steel alloy and its surroundings in very small quantities compared to the environment[5-8]. Most corrosion inhibitors act through adsorption, retarding the cathodic, anodic or both electrochemical corrosion reactions. Inhibition mechanism and efficiency vary due to several factors e.g. concentration, pH, acid anion and type of metal. Most promising inhibitors are organic compounds that contain heteroatoms which chemically adsorbed onto metallic surfaces. Research on organic derivatives of benzonitrile has proven their corrosion inhibition effectiveness however only in low molar concentrations of acid media[9-13]. This research evaluates the corrosion inhibiting action of benzonitrile on 420 martensitic stainless in 6M H_2SO_4 acid solution.

MATERIAL AND METHODS

420 stainless steel (HT-420ST) procured from the open market has the following percentage content of alloying elements after analysis; shown in Table 1. The steel samples are of cylindrical dimension with an unconcealed area of 0.79 cm^2 after embedding in resin mounts. HT-420ST samples were cut and sectioned before being abraded with silicon carbide papers (80, 320, 600, 800 and 1000 grits). They were thereafter washed with distilled water and acetone for electrochemical tests according to ASTM G1 – 03[14]. HT-420ST samples were heat heated in a muffle furnace to 1000°C before quenching in distilled water. The furnace temperature was controlled at an accuracy ± 10°C coupled with thermocouple (K-Type). Benzonitrile (BEZT) shown in Fig. 1 was procured from BOC Sciences, USA. is a achromatic organic liquid with a sweet almond odour. It has a density of 103.12 g/mol and a chemical formula of C_7H_5N. BEZT was prepared in quantitative concentrations of 9.25 x 10^3, 1.85 x 10^2, 2.77 x 10^2, 3.70 x 10^2 and 4.62 x 10^2 in 400 mL of 6 M H_2SO_4 acid prepared from standard grade (98% purity) with distilled water. Electrochemical evaluation through polarization was performed out at 34°C with a triple electrode cell system, consisting of 200 mL of the electrolyte and HT-420ST electrodes connected to Digi-Ivy 2311 potentiostat. Graphical plots were produced at a scan rate of 0.0015 V/s from -1.5 V and +1.5 V. The acid inhibitor solution, before and after polarization tests were subjected to infrared ray beams using Bruker Alpha FTIR spectrometer from 375 to 7500 cm^{-1} wavelength and 0.9 cm^{-1} resolution. Graphical plots of ATF-FTIR absorption including of spectra peaks were evaluated and correlated with theoretical ATF-FTIR absorption Table for identification of functional groups involved in the corrosion inhibition of HT-420ST.

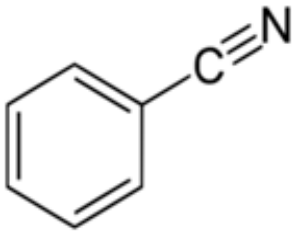

Fig. 1. Molecular structure of benzonitrile

RESULTS AND DISCUSSION

Potentiodynamic polarization studies

Graphical illustrations of HT-420ST potentiodynamic polarization curves in 6M H_2SO_4 solution at 0% - 0.63% BEZT concentration are depicted in Fig 2, while the results of the polarization test are given in Table 2. HT-420ST at 0% BEZT concentration exhibited a corrosion rate value of

Table 1: Percentage content of alloying elements in HT-420ST

Element	C	Mn	P	S	Si	Cr	Ni	Mb	N	Fe
% Composition	0.28	0.8	0.04	0.02	0.8	14	0.4	-	-	79.15

3.30 mm/y, analogous to corrosion current density of 3.04 x 10^4 Acm^2. This value is significantly higher than the corrosion rates of HT-420ST at 0.13% - 0.63% BEZT due to the activity of SO_4^{2-} ions in the aqueous media. The strong ionization potential of 6M H_2SO_4 in H_2O at 0% BEZT causes the release two protons which aggressively reacts with and deteriorates HT-420ST surface. Observation of the anodic-cathodic polarization plot of HT-420ST at 0% BEZT shows strong deviation from the plots obtained at 0.13% - 0.63% BEZT due to corrosion and accelerated destruction of the passive film.

Table 2: Results of HT-420ST potentiodynamic polarization behaviour in 6 M H_2SO_4 solution at 0% - 0.63% BEZT concentration

Sample	BEZT Conc. (%)	BEZT Conc. (M)	HT-420ST Corrosion Rate (mm/y)	BEZT Inhibition Efficiency (%)	Corrosion Current (A)	Corrosion Current Density (A/cm^2)	Corrosion Potential (V)	Polarization Resistance, Rp (Ω)	Cathodic Tafel Slope, Bc (V/dec)	Anodic Tafel Slope, B_a (V/dec)
A	0	0	3.30	0	2.40E-04	3.04E-04	-0.306	107.10	-10.50	8.06
B	0.13	9.25E-03	0.19	99.40	1.35E-05	1.71E-05	-0.274	1906.00	-9.23	20.97
C	0.25	1.85E-02	0.19	99.39	1.37E-05	1.74E-05	-0.267	1874.00	-7.58	23.03
D	0.38	2.77E-02	0.21	99.32	1.52E-05	1.92E-05	-0.282	1693.00	-7.25	17.36
E	0.50	3.70E-02	0.33	98.93	2.40E-05	3.03E-05	-0.285	1073.00	-7.77	16.27
F	0.63	4.62E-02	0.22	99.29	1.59E-05	2.02E-05	-0.348	1612.00	-9.68	9.28

This also shows BEZT alters the mechanism of electrochemical reactions responsible for HT-420ST corrosion through adsorption, surface coverage, and suppression of the reduction reactions.

Addition of BEZT (0.13% - 0.63% BEZT) to the acid solution significantly altered the corrosion resistance properties of HT-420ST as shown from the changes in corrosion potential values from -0.306 V at 0% BEZT to -0.274 V at 0.13% BEZT due to anodic inhibition through surface coverage and precipitation of BEZT on reactive sites on the steel surface. Changes in BEZT concentration had no effect on it inhibition efficiency confirming the inhibitor to be concentration dependent. BEZT caused a more significant change in the anodic Tafel slope than the cathodic counterpart from comparison of Tafel slope values at 0% and 0.13% - 0.63% BEZT due to its higher anodic exchange-current density. The visible change in anodic Tafel slope values after 0% BEZT is due to changes in the electrode substrate, rate controlling step and influence of potential controlled conditions. This is consistent with the earlier observation of the corrosion potential values. The maximum change in corrosion potential with respect to the value at 0% BEZT is less than 85 mV as a result BEZT is a mixed type inhibitor with dominant anodic inhibiting properties.

Mechanism of Inhibition

BEZT consist of a 5-membered 1, 3-thiazole ring fused to a benzene ring. The presence of heteroatoms of N and S, and π-electrons on the thiazole rings of BEZT strongly influences its adsorption and mode of interaction with HT-420ST surface, and the resulting formation of metallic complexes. The lone pair of electrons in the heteroatoms within BEZT molecules facilitates transfer of electrons from BEZT to the metal. The S atom enables the formation of dπ-dπ bond resulting from the overlapping of 3d-electrons, while the double bonds in BEZT molecule reverse release of metal d-electron to the π-orbital. The wide variation in corrosion rate values of HT-420ST before and after BEZT inhibition shows that HT-420ST strongly oxidizes in 6M H_2SO_4 solution releasing metallic cations. This behaviour results in vacant'd' orbital of the iron substrate metal leading to the formation of co-ordination bond between Fe–N-S, hence adsorption. Electrostatic attraction occurs between

BEZT inhibitor and HT-420ST; the positively charged HT-420ST surface electrostatically attracts SO_4^{2-} ions, which preadsorbed onto steel surface. The excess negative charge draws cationic BEZT molecules forming a protective ($FeSO_4^{2-}$BEZT-H^+)ad layer. BEZT cations are also attracted to cathodic sites on HT-420ST surface, competing with H- ions for reduction, hence stifling the hydrogen evolution reaction.

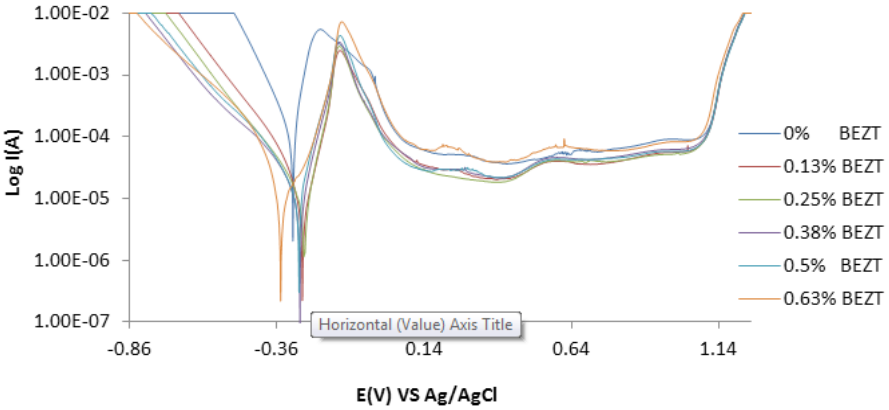

Fig. 2. Graphical plot of the anodic-cathodic polarization curves for HT-420ST at 6M H2SO4/0% - 0.63% BEZT

ATF-FTIR Spectroscopy analysis

Functional groups within BEZT molecules i.e. atoms and bonds responsible for electrostatic attraction, molecular adsorption and invariably corrosion inhibition of HT-420ST surface were identified by ATF-FTIR spectroscopy and correlated with the ATR-FTIR Theoretical Table[15, 16]. Fig. 3 shows the spectra plots of the 6 M H_2SO_4 /BEZT solutions before and after HT-420ST corrosion. The transmittance of the spectra plot of 6 M H_2SO_4/BEZT before corrosion decreased significantly after the corrosion test by comparison with the transmittance of the spectra plot of 6 M H_2SO_4/BEZT after corrosion at wavelengths between of 526 - 673 cm^{-1}, 826 - 1030 cm^{-1}, 1360 - 1433 cm^{-1}, 1529 - 1597 cm^{-1}, 1776 - 2822 cm^{-1} and 3004 - 3489 cm^{-1} due to corrosion inhibition resulting from adsorption of specific BEZT functional groups. The identified moieties are alkynes, aromatics, primary, secondary amines, carboxylic acids, alkenes, alkanes, nitro compounds, aldehydes, alkynes (terminal), amides and alcohols, phenols which all consists of bonds such as –C(triple bond)C–H: C–H bend, C–H "oop", N–H wag, O–H bend, =C–H bend, C–H rock, C–C stretch (in–ring), N–O asymmetric stretch, N–H bend, H–C=O: C–H stretch, =C–H stretch, C–H stretch, –C(triple bond) C–H: C–H stretch, N–H stretch, O–H stretch and H–bonded. The decrease in transmittance at the specific wavelength range confirmed the surface coverage effect and adsorption of BEZT compound on HT-420ST resulting on MCS surface.

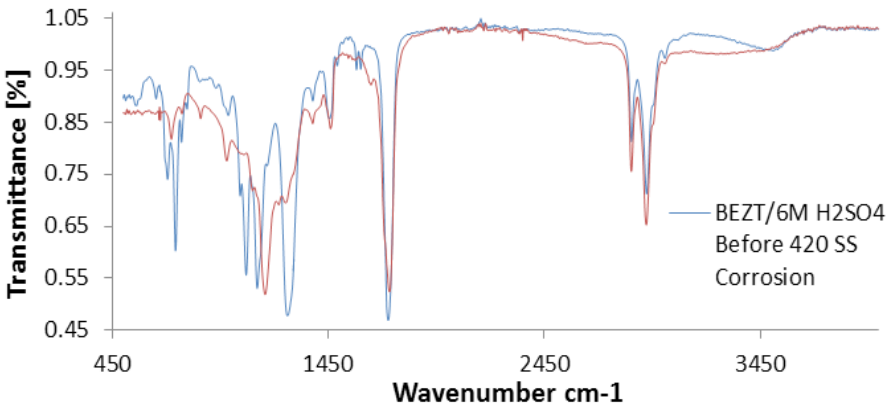

Fig. 3. ATF-FTIR spectra of BEZT/6M H_2SO_4 before and after HT-420ST corrosion inhibition

Adsorption Isotherm

BEZT adsorption on HT-420ST surface was further determined and studied through adsorption models. Studies show BEZT agrees with the Langmuir and Freundlich isotherm at correlation coefficients of 1 and 0.7570 respectively. Langmuir isotherm plot of C_BEZT/θ versus CBEZT [Fig. 4(a)], calculated from equation 1 assumes that; (i) The molecular interactions at the metal- solution interface is constant, (ii) Gibbs free energy results (equation 3) is non-dependent on the extent of molecular protection and (iii) The effect of interaction of adsorbates on the value of Gibbs free energy is negligible[17]. The Frumkin plot of Log θ/(1-θ) versus θ [Fig. 4(b)], determined from equation 2 proposes complete adsorbate covering at peak BEZT concentrations for a non-disparate alloy surface coupled with negligible effect of lateral interaction.

$$\theta = \left[\frac{K_{ads}\, C_{BEZT}}{1 + K_{ads}\, C_{BEZT}}\right] \quad (1)$$

$$\text{Log}\,[C_{BEZT} * (\theta/_{1-\theta})] = 2.303 \log K_{ads} + 2\alpha\theta \quad (2)$$

Thermodynamics of the corrosion inhibition

The stability of molecular interaction with respect to BEZT adsorption on HT-420ST is equivalent to the quantity of H_2O molecules (n) substituted by BEZT molecules in the acid solution. This is directly equivalent to the amount of HT-420ST cations released into the acid solution, and degree of BEZT coverage. Data for Gibbs free energy (ΔG_{oads}) for the molecular interaction are shown in Table 3 and were calculated from the mathematical relationship below[18].

$$\Delta G_{ads} = -\ 2.303RT \log [55.5K_{ads}] \quad (3)$$

55.5 is a constant for standard water concentration in the acid media, *R* represents the universal gas constant, *T* stands for the absolute temperature and K_{ads} is the equilibrium constant of adsorption. K_{ads} is related to surface coverage (θ) from the Langmuir equation (equation 1).

The surface properties and non-homogeneous nature of HT-420ST strongly influences the ΔGoads values of BEZT adsorption with respect to the extent of BEZT coverage value. Negative values of $\Delta G°_{ads}$ identifies the spontaneous behaviour of the adsorption species on the metal surface. The highest $\Delta G°_{ads}$ value obtained for BEZT adsorption on HT-420ST is -42.22 KJmol^{-1} at 2.5% BEZT, while the lowest value in both acids are -38.89 KJmol^{-1} at 1.5% BEZT and -41.53 KJmol^{-1} at 6.5% BEZT. This observation is consistent with chemisorption adsorption mechanism[19, 20].

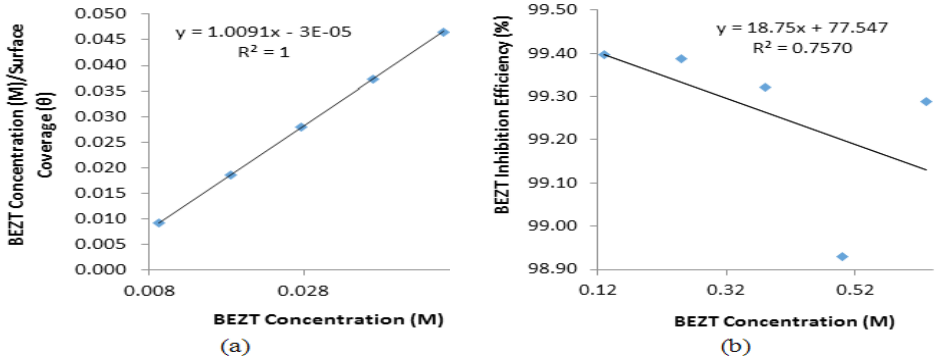

Fig. 4. Graphical plot of (a) C/θ versus BEZT concentration, (b) θ/(1-θ) versus BEZT concentration in 6M H_0SO_4

Table 3: Result for Gibbs free energy ($\Delta G°_{ads}$), surface coverage (θ) and equilibrium constant of adsorption (K_{ads}) for BEZT adsorption on HT-420ST in 6 M H_2SO_4

HT-420ST Samples	BEZT Concentration (M)	Surface Coverage (θ)	Equilibrium Constant of adsorption (K_{ads})	Gibbs Free Energy, ΔG_{ads} (Kjmol^{-1})
A	0	0	0	0
B	9.25E-03	0.994	17838.8	-34.21
C	1.85E-02	0.994	8768.9	-32.45
D	2.77E-02	0.993	5276.3	-31.19
E	3.70E-02	0.989	2498.3	-29.34
F	4.62E-02	0.993	3013.8	-29.80

CONCLUSION

Benzonitrile inhibited the corrosion of 420 martensitic steel in 6M H_2SO_4 solution through surface coverage and chemisorption molecular interaction according to the Langmuir and Freundlich isotherm model from potentiodynamic polarization and ATF-FTIR spectroscopy. The chemical compound formed a protective barrier film on the steel inhibiting the electrolytic transport and adsorption of SO_4^{2-} responsible for corrosion. The compound was determined to be mixed type with dominant anodic inhibition effect from Tafel slope analysis.

ACKNOWLEDGEMENT

The author is greatful to Covenant University Ota, Ogun State, Nigeria for the sponsorship and provision of research facilities for this project.

REFERENCES

1. El-Etre, A.Y. *Corros. Sci.,* **1998**, *40*(11), 1845-1850.
2. El-Etre, A.Y.; Abdallah, M. *Corros. Sci.*, **2000**, *42*(4), 731-738.
3. Parikh, K.S.; Joshi, K. *J. Trans. SAEST.*, **2004**, *38*(1-2), 29-35.
4. Loto, R.T.; Aiguwurhuo, O.; Evana, U. *Rev. Téc. Ing. Univ. Zulia.*, **2016**, *39*(7), 35-40.
5. Tantawy, N. The *Annals of University, Dunarea de Jos of Galati Fascicle.*, **2005**, *8*, 112-114.
6. Ahmad, I.; Rahuma, M.N.; Knish, A. *J. of Pharm. & Chem. Sci.*, **2014**, *3*(1), 255-259.
7. Loto, C.A.; Joseph, O.O.; Loto, R.T.; Popoola, A.P. I. *Int. J. Electrochem. Sci.*, **2014**, *9*, 1221-1231.
8. Loto, C.A.; Loto, R.T. *Int. J. Electrochem. Sci.* **2013**, *8*, 12434-12450.
9. Fouda, A.S.; El-Azaly, A.H.; Awad, R.S.; Ahmed, A.M. *Int. J. Electrochem. Sci.*, **2014**, *9*, 1117-1131.
10. Agrawal, R.; Namboodhiri, T. K.G. *J. of Appl. Elect.*, **1997**, *27*(11), 1265-1274.
11. Zaiz, T.; Lanez, T. *J. of Fund. & Appl. Sci.*, **2012**, *4*(2). http://dx.doi.org/10.4314/jfas.v4i2.8.
12. Saha S.K.; Dutta, A.; Ghosh, P.; Sukulc, D.; Banerjee, P. *Phys. Chem. Chem. Phys.*, **2016**, *27*(18), 17898-17911.
13. Loto, R.T. *Sci. Rep.*, **2012**, *7*, 17555. doi: 10.1038/s41598-017-17867-0
14. ASTM G1 – 03 (2011). Standard Practice for Preparing, Cleaning, and Evaluating Corrosion Test Specimens. http://www.astm.org/Standards/G1.
15. Table of Characteristic IR Absorptions. http://orgchem.colorado.edu/Spectroscopy/specttutor/irchart.pdf.
16. George, S. Infrared and Raman Characteristic Group Frequencies: Tables and Charts. John Wiley & Sons, New York, **2004**.
17. Ashish, K.S.; Quraishi, M.A. *Corros. Sci.*, **2011**, *53*(4), 1288-1297.
18. Soror, T.Y. *J. of Mats. Sci. & Tech.*, **2014**, *20*(4), 463-466.
19. Bouklah, M.; Hammouti, B.; Lagrene, M.; Bentiss, F. *Corros. Sci.*, **2006**, *48*(9), 2831-2842.
20. Loto, R.T. *Cogent Eng.*, **2016**, *3*, 1242107. https://doi.org/10.1080/23311916.2016.1242107.